

# Dynamin Interacts with Members of the Sumoylation Machinery\*

Received for publication, March 16, 2004, and in revised form, April 30, 2004  
Published, JBC Papers in Press, April 30, 2004, DOI 10.1074/jbc.M402911200

Ram Kumar Mishra<sup>‡</sup>, Shashidhar S. Jatiani<sup>‡</sup>, Ashutosh Kumar<sup>§</sup>, Venkateswara Rao Simhadri<sup>‡</sup>,  
Ramakrishna V. Hosur<sup>§</sup>, and Rohit Mittal<sup>‡¶</sup>

From the Departments of <sup>‡</sup>Biological Sciences and <sup>§</sup>Chemical Sciences, Tata Institute of Fundamental Research, Mumbai 400 005, India

**Dynamin is a GTP-binding protein whose oligomerization-dependent assembly around the necks of lipid vesicles mediates their scission from parent membranes. Dynamin is thus directly involved in the regulation of endocytosis. Sumoylation is a post-translational protein modification whereby the ubiquitin-like modifier Sumo is covalently attached to lysine residues on target proteins by a process requiring the concerted action of an activating enzyme (ubiquitin-activating enzyme), a conjugating enzyme (ubiquitin carrier protein), and a ligating enzyme (ubiquitin-protein isopeptide ligase). Here, we show that dynamin interacts with Sumo-1, Ubc9, and PIAS-1, all of which are members of the sumoylation machinery. Ubc9 and PIAS-1 are known ubiquitin carrier protein and ubiquitin-protein isopeptide ligase enzymes, respectively, for the process of sumoylation. We have identified the coiled-coil GTPase effector domain (GED) of dynamin as the site on dynamin that interacts with Sumo-1, Ubc9, and PIAS-1. Although we saw no evidence of covalent Sumo-1 attachment to dynamin, Sumo-1 and Ubc9 are shown here to inhibit the lipid-dependent oligomerization of dynamin. Expression of Sumo-1 and Ubc9 in mammalian cells down-regulated the dynamin-mediated endocytosis of transferrin, whereas dynamin-independent fluid-phase uptake was not affected. Furthermore, using high resolution NMR spectroscopy, we have identified amino acid residues on Sumo-1 that directly interact with the GED of dynamin. The results suggest that the GED of dynamin may serve as a scaffold that concentrates the sumoylation machinery in the vicinity of potential acceptor proteins.**

The protein dynamin is an important component of the endocytic machinery in cells (1, 2). Dynamin isoforms are thought to mediate their functions by virtue of their ability to aid in the scission of vesicles from membranes (3). Mammalian dynamin-1 and dynamin-2 have been shown to have a role in the scission of clathrin-coated vesicles and in the budding of caveolae (4). The dynamin family can be considered to include classical dynamins as well as the dynamin-like mitochondrial division proteins Dnm1, Mgm1, and Fzo1 and the interferon-inducible Mx and guanylate-binding proteins, which have been

shown to possess antiviral activities (5). The yeast Vps1 and plant ARC5 and ADL proteins also belong to this family of GTP-binding proteins (6). True dynamins are modular proteins characterized by the presence of an N-terminal GTP-binding domain, a contiguous “middle domain” of ill defined function, and a lipid-binding pleckstrin homology (PH)<sup>1</sup> domain, followed by a coiled-coil “assembly” domain and a proline-rich domain (PRD). Other dynamin-like proteins, e.g. Mx, lack the pleckstrin homology and proline-rich domains. The GTPase domain is the most highly conserved domain within members of the dynamin family. The coiled-coil assembly domain has been shown to mediate the assembly of dynamin into oligomers (7) and has also been shown to possess an assembly-stimulated GTPase-accelerating property for the GTPase domain. The oligomerization of dynamin is critical for its function in mediating the process of endocytosis (8). Dynamin-mediated endocytosis is critical for synaptic vesicle recycling in the central nervous system and for cell-surface receptor endocytosis in all cells of an organism. GTP-bound dynamin is thought to assemble in the form of rings around the necks of budding vesicles; a conformational change in the dynamin collar is currently thought to aid the scission of the vesicle from the parent membrane. Dynamin may be considered to catalyze this change either by recruiting effector enzymes like endophilin (9, 10) that have lipid-modifying activity or by an intrinsic mechanochemical function (11). Whatever the exact mode of dynamin function in the facilitation of endocytic vesicle scission, it is clear that the assembly and GTP-binding properties of dynamin are critical to the process of endocytosis *in vivo*.

Dynamin mediates endocytosis in concert with various other molecules, *viz.* amphiphysin, endophilin, etc. Almost all the currently identified dynamin-interacting molecules engage the C-terminal PRD of dynamin. The other domains of dynamin are also known to participate in dynamin function by mediating intramolecular interactions within the dynamin molecule and/or intermolecular interactions within dynamin homo-oligomers. The middle domain has been shown to interact with the coiled-coil GTPase effector domain (GED) of dynamin (12). The GED is also known to interact with the N-terminal GTP-binding domain of dynamin (13) and to act as an internal GTPase-activating factor for dynamin. In addition, the GED is thought to interact with the GED of other dynamin molecules, aiding oligomerization of dynamin (8). The PH domain of dy-

\* This work was supported by an intramural grant from the Tata Institute of Fundamental Research and a grant from the Department of Science and Technology, India. The costs of publication of this article were defrayed in part by the payment of page charges. This article must therefore be hereby marked “advertisement” in accordance with 18 U.S.C. Section 1734 solely to indicate this fact.

¶ To whom correspondence should be addressed: Dept. of Biological Sciences, Tata Inst. of Fundamental Research, Homi Bhabha Rd., Mumbai 400 005, India. Tel.: 91-22-2280-4545; Fax: 91-22-2280-4610; E-mail: mittal@tifr.res.in.

<sup>1</sup> The abbreviations used are: PH, pleckstrin homology; PRD, proline-rich domain; GED, GTPase effector domain; SH3, Src homology 3; E1, ubiquitin-activating enzyme; E2, ubiquitin carrier protein; E3, ubiquitin-protein isopeptide ligase; SD, synthetic dropout; oNPG, *o*-nitrophenyl- $\beta$ -D-galactopyranoside; GST, glutathione *S*-transferase; GFP, green fluorescent protein; CHO, Chinese hamster ovary; HSQC, heteronuclear single quantum correlation spectroscopy; NOESY, nuclear Overhauser effect correlation spectroscopy; MAPK, mitogen-activated protein kinase; MEK, mitogen-activated protein kinase/extracellular signal-regulated kinase kinase.

namin interacts with phosphatidylinositol lipids, thereby targeting dynamin to the plasma membrane (14), and may also interact with the  $\beta\gamma$ -subunit complex of heterotrimeric GTP-binding proteins (15). Additionally, the function of dynamin is potentially regulated by phosphorylation by multiple kinases (16). The PRD of dynamin contains many sites that engage SH3 domains. The SH3 domains of the tyrosine kinase pp60<sup>src</sup>, amphiphysin, endophilin, Grb2, intersectin, Abp1, syndapin, mixed lineage kinase, p85, phospholipase C $\gamma$ , and phosphatidylinositol 3-kinase are known to interact with the PRD of dynamin (17). Additional non-SH3 interactors of dynamin are  $\alpha$ -adaptin (18) and nucleoside-diphosphate kinase (19). Recently, auxilin and Hsc70 have been identified as the first non-PRD interactors of dynamin (20).

This study was designed to uncover hitherto unidentified interactors of dynamin using yeast two-hybrid analysis (21). We biased our search by using dynamin lacking the C-terminal PRD (dynamin $\Delta$ PRD) as bait in the yeast two-hybrid screen. A human brain cDNA library was used to screen for interactors of dynamin $\Delta$ PRD. This has led to the identification of several putative interactors of dynamin. Here, we characterize the interaction of dynamin with members of the sumoylation cascade. Sumoylation is a post-translational modification mechanistically similar to ubiquitination. Sumo (small ubiquitin-related modifier) is a 101-amino acid protein that has the potential (like ubiquitin) to covalently attach to lysine side chains in target molecules (22–25). This covalent attachment of Sumo is mediated by a cascade of enzymes known as the E1 (activating), E2 (conjugating), and E3 (ligating) enzymes. The 101-amino acid Sumo polypeptide is proteolytically processed by a C-terminal hydrolase to a 97-amino acid moiety ending in a diglycine motif. This mature form of Sumo forms a thiol ester linkage with a cysteine residue in the activating E1 enzyme (the SAE1/2 heterodimer in humans) and is subsequently transferred to the E2 enzyme (Ubc9) to form another thiol ester linkage. The activated Sumo is ultimately attached to an available lysine residue in an acceptor polypeptide through the formation of an isopeptide bond between the C-terminal glycine residue of Sumo and an  $\epsilon$ -amino group of the lysine. This last step often requires the participation of E3 ligases, three of which PIAS (protein inactivator of activated STAT proteins), RanBP2, and Pc2 are currently known to participate in the process of sumoylation (26).

Several proteins that are not known to be sumoylated are known to interact with Sumo. There are reports of noncovalent interaction of the nucleocapsid proteins of the Tula and Hantaan hantaviruses with Sumo-1 (27, 28). Also, noncovalent association of Sumo-1 with the Rad51 and Rad52 proteins has been shown to have a regulatory role in homologous recombination in mammalian cells (29).

In this study, we show that the endocytic protein dynamin interacts noncovalently with members of the sumoylation machinery and that this interaction inhibits the oligomerization of dynamin. Consistent with this effect, we found that overexpression of Sumo in mammalian cells abrogates dynamin-dependent endocytosis. We have narrowed down the region of interaction with the sumoylation machinery to be the GED of dynamin and, by high resolution structural mapping using NMR, identified the amino acid residues on Sumo-1 responsible for the interaction.

#### EXPERIMENTAL PROCEDURES

**Cloning of Bait**—Amino acids 1–753 of human dynamin-1 were PCR-amplified from pTMI-hDyn1 (provided by Dr. Alexander van der Blik, UCLA) using primers 5'-(CCCGAATTCATGGGCAACCGCGG-C-3' and 5'-GCGGAAGCTTGGGCGTGTGACGG-3'. The PCR product was digested with EcoRI and HindIII and ligated into the pBS-SK vector between the EcoRI and HindIII sites. From here, the dynamin-

$\Delta$ PRD cDNA was excised using EcoRI and SalI and subcloned into the pLexA yeast expression vector (Clontech). The construct was confirmed by multiple restriction digests and DNA sequencing. This clone was used for screening a human brain cDNA library cloned into the pB42AD vector (Clontech). Other control plasmids and the host yeast strain were also provided in the Matchmaker yeast two-hybrid kit procured from Clontech.

**Yeast Two-hybrid Screening**—The yeast strain supplied with the kit and used in this study is EGY48 (*MAT $\alpha$* , *his3*, *trp1*, *ura3*, *LexA<sub>op(x6)</sub>-LEU2*), a reporter host strain carrying a wild-type *LEU2* gene under the control of LexA operators. Yeast cells were grown or maintained in YPD medium (1% yeast extract, 2% Bacto-peptone, and 2% glucose) or synthetic dropout (SD) medium lacking the appropriate nutrients to maintain the selection. Yeast cells were transformed using the polyethylene glycol/lithium acetate method as described (30). First, EGY48 cells were transformed with the p8oplacZ plasmid ( $\beta$ -galactosidase reporter plasmid), and the transformants were maintained on SD/Glu/Ura<sup>-</sup> plates. For transformation of the bait plasmid, EGY48(p8oplacZ) colonies were grown in SD/Glu/Ura<sup>-</sup> medium and subcultured later in YPD medium. Using the polyethylene glycol/lithium acetate method, competent cells were made and transformed with 1  $\mu$ g of pLexA-hDyn $\Delta$ PRD and 60  $\mu$ g of salmon sperm DNA. These transformants were selected and maintained on SD/Glu/Ura<sup>-</sup>/His<sup>-</sup> plates. For library screening, the target plasmid library was sequentially transformed into EGY48-(p8oplacZ+pLexA-hDyn $\Delta$ PRD). Library DNA corresponding to  $3 \times 10^6$  colony-forming units was transformed, and positive clones were screened on SD/Gal/raffinose/Ura<sup>-</sup>/His<sup>-</sup>/Trp<sup>-</sup>/Leu<sup>-</sup> plates. The positive clones obtained were further narrowed in number by control transformations, and final clones were examined for *lacZ* reporter gene expression using a colony lift filter assay.

**Isolation and Characterization of Positive Clones**—Plasmid DNA was extracted from yeast cells using glass beads, and positive clones in the pB42AD vector were rescued by transforming the DNA into *Escherichia coli* strain KC8. (This strain has a defect in *trpC*, which can be complemented by the *TRP1* gene in pB42AD.) Clones thus obtained were sequenced for their identity and re-tested in yeast two-hybrid assays for interaction with the human dynamin- $\Delta$ PRD bait plasmid. Using NCBI BLAST, the identity of each clone was assigned. The screen yielded full-length Sumo-1 and PIAS-1-(396–651) cloned into the pB42AD plasmid. The cDNA for Ubc9 (obtained from Prof. Ronald T. Hay, University of St. Andrews, St. Andrews, Scotland) was amplified using primers 5'-CCCGAATTCATGTCGGGGATCGC-3' and 5'-CCGCTCGAGTAT-GAGGGCGCAAACCTTCTTGG-3' and cloned into the EcoRI/XhoI-cut pB42AD yeast expression vector.

**o-Nitrophenyl- $\beta$ -D-galactopyranoside (oNPG) Assay**—The strength of protein-protein interactions observed in yeast cells was quantitated by oNPG assays as described below. 5 ml of cultures for yeast cotransformants were grown overnight in SD medium + 2% glucose, subcultured in 3 ml of SD medium + 2% galactose and 1% raffinose with 5% inoculum, and allowed to grow at 30 °C for 8–10 h. oNPG assays were performed in the  $A_{600 \text{ nm}} \sim 0.5$ –1.0 range following the Clontech protocol. Briefly, cells were pelleted and washed with 1.5 ml of Z buffer (16.1 g/liter Na<sub>2</sub>HPO<sub>4</sub>·7H<sub>2</sub>O, 5.5 g/liter NaH<sub>2</sub>PO<sub>4</sub>·H<sub>2</sub>O, 0.75 g/liter KCl, 0.246 g/liter MgSO<sub>4</sub>·7H<sub>2</sub>O, pH 7.0) and later resuspended in 300  $\mu$ l of Z buffer. 100  $\mu$ l of resuspended cells were aliquoted in fresh tubes and subjected to three freeze/thaw cycles. To these tubes were added 700  $\mu$ l of Z buffer + 0.27%  $\beta$ -mercaptoethanol and 160  $\mu$ l of oNPG (4 mg/ml), followed by incubation at 30 °C for color development. 400  $\mu$ l of 1 M Na<sub>2</sub>CO<sub>3</sub> were added to stop the reaction. Color development in the supernatant was measured at  $A_{420 \text{ nm}}$  after centrifuging the tubes at full speed in a microcentrifuge for 10 min.

**Interaction of Dynamin with Sumo-1, Ubc9, and PIAS-1**—The cDNA for Sumo-1 flanked by BamHI and XhoI sites was amplified and ligated into the pGEXKG vector. This was used to express GST-Sumo-1 in bacteria. GST-PIAS-(396–651) was expressed in bacteria from pGEX-4T1 into which amino acids 396–651 of PIAS-1 amplified from pB42AD-PIAS with flanking EcoRI and XhoI sites had been ligated. The plasmid pGEX-2T-hUbc9 expressing GST-Ubc9 was a kind gift of Prof. Ronald T. Hay. For pull-down assays, GST fusion proteins were expressed in *E. coli* BL21 cells and immobilized on glutathione-Sepharose 4B beads (Amersham Biosciences); the beads were then incubated with bovine serum albumin (100  $\mu$ g/ml) to block unreacted sites on the beads. Rat brain lysate was prepared by homogenizing 0.3–0.5 g of rat brain tissue in 2.5 ml of Tris-buffered saline (50 mM Tris (pH 7.4) and 150 mM NaCl) containing protease inhibitors in a Dounce homogenizer and spinning the suspension at 20,800  $\times g$  for 35 min at 4 °C. The clear supernatant thus obtained was used as rat brain lysate. In a typical pull-down reaction,  $\sim 20 \mu$ g of recombinant protein-coated beads were

incubated with 200–300  $\mu$ l of rat brain lysate for 30 min with end-over-end rotation at 4 °C. Beads were washed with Tris-buffered saline, 0.1% bovine serum albumin, and 0.1% Triton X-100; boiled in 5 $\times$  Laemmli buffer; and resolved on 10% SDS-polyacrylamide gel. The gel was processed for Western transfer, and the membranes were probed with anti-dynamin-1 antibodies (Santa Cruz Biotechnology) and developed using ECL (Amersham Biosciences).

**GTP Hydrolysis Assays**—GTP hydrolysis by dynamin was assessed using [ $\gamma$ - $^{32}$ P]GTP. Dynamin from rat brain was purified by virtue of its affinity for the SH3 domain of amphiphysin by the method of Stowell *et al.* (11). For assembly-stimulated GTPase assays, 0.2  $\mu$ M dynamin in TMND buffer (20 mM Tris (pH 7.4), 5 mM MgCl<sub>2</sub>, 150 mM NaCl, and 1 mM dithiothreitol) was incubated with 50  $\mu$ g/ml phosphatidylserine (Serva Feinbiochemica, Heidelberg, Germany) for 30 min on ice. Various amounts of Sumo-1 or Ubc9 were then added to the mixture, which was further incubated for 30 min on ice. GTP hydrolysis was initiated by the addition of 200  $\mu$ M GTP (containing [ $\gamma$ - $^{32}$ P]GTP) and allowed to proceed for 30 min at room temperature. The total reaction volume was 75–100  $\mu$ l. The reaction was stopped by the addition of 600  $\mu$ l of acidified 7% charcoal slurry, and the extent of GTP hydrolysis was measured by counting P<sub>i</sub> release in a liquid scintillation counter (Packard Instrument Co.). Incubation of dynamin with Sumo-1 or Ubc9 before the addition of phosphatidylserine showed the same results.

**Oligomerization Assays**—Oligomerization of Dynamin was assessed by the sedimentation assay (31). Dynamin, phosphatidylserine, and either Sumo-1 or Ubc9 were incubated as described above in TMND buffer. The reactions (total volume of 150  $\mu$ l) were then centrifuged for 15 min at 100,000  $\times$  *g* in a Beckman Ti-42.2 rotor at 4 °C. The supernatants were precipitated with 10% trichloroacetic acid, and the total protein from the supernatant and pellet fractions was then visualized by 10% SDS-PAGE and Coomassie Blue staining. The Sumo-1 and Ubc9 proteins used in the oligomerization and GTPase assays were expressed in *E. coli* as hexahistidine-tagged proteins expressed from the pQE32 (QIAGEN Inc.) and pET28a(+) (Novagen) vectors, respectively.

**Expression of Sumo-1 and Ubc9 in Mammalian Cells**—The cDNA for Sumo-1 was PCR-amplified with BamHI and XhoI ends and ligated into the pcDNA3 vector. The resultant pcDNA3-Sumo-1 clone was digested with SacI to subclone Sumo-1 into the GFP expression vector pEG-FPC1. Ubc9 was amplified with EcoRI and XhoI ends and ligated into the pcDNA3 vector. The resultant pcDNA3-Ubc9 clone was digested with EcoRI and XhoI to subclone Ubc9 into the EcoRI and SalI sites of the pEGFPC2 vector to yield GFP-Ubc9. For rescue experiments, a pcDNA3 construct of full-length rat dynamin-1 (a gift of Dr. Pietro de Camilli, Yale University) was used. pcDNA3-c-Myc was prepared by inserting a linker encoding the c-Myc epitope into the HindIII and BamHI sites of the pcDNA3 vector. The GED (EcoRI/SalI fragment) was subcloned between the EcoRI and XhoI sites of pcDNA3-c-myc.

The Chinese hamster ovary (CHO) cell line TRVb-1 (with the hamster transferrin receptor knocked out and stably expressing the human transferrin receptor) (32) was maintained in Ham's F-12 medium supplemented with 5% fetal bovine serum, 100  $\mu$ g/ml streptomycin, 100 units/ml penicillin, and 100  $\mu$ g/ml Geneticin. Cells were plated on poly-D-lysine-coated 35-mm dishes (with cover-slip bottoms) 36 h before transfection. Cells were transfected using FuGENE 6 transfection reagent (Roche Applied Science) with 1.0  $\mu$ g of DNA following the manufacturer's instructions. 24–36 h post-transfection, cells were assayed for internalization of fluorescently labeled transferrin or RNase A.

**Endocytosis Assays**—Alexa 568-conjugated transferrin was made up to 10.5 ng/ml in labeling medium (Ham's F-12 medium containing, 0.3 mg/ml NaHCO<sub>3</sub>, 5% fetal bovine serum, and 15 mM HEPES (pH 7.2)). Transfected TRVb-1 cells were incubated with Alexa 568-conjugated transferrin for 30 min at 37 °C. Cells were then cooled on ice, and the excess label was washed with ice-cold buffer A (150 mM NaCl, 5 mM KCl, 1 mM CaCl<sub>2</sub>, 1 mM MgCl<sub>2</sub>, and 20 mM HEPES (pH 7.4)). Fluorescent transferrin was removed from its receptor at the cell surface by multiple washes with ice-cold acid rinse buffer containing 25.5 mM citric acid, 24.5 mM trisodium citrate, 280 mM sucrose, and 0.01 mM deferoxamine mesylate (pH 4.0). Cells were fixed at room temperature with 2.5% paraformaldehyde in buffer A for 20 min, rinsed twice with buffer A, and used for imaging.

RNase A internalization assays were performed as described (33). Briefly, Alexa 555-conjugated RNase A was made up to 10  $\mu$ M in labeling medium. Transfected cells were incubated with labeled RNase A for 5 min at 37 °C. Cells were cooled on ice, washed twice with ice-cold buffer A, and fixed as described above.

**Microscopy and Image Processing**—Confocal imaging was carried out on a Bio-Rad Radiance 2100 confocal microscope equipped with a Nikon Eclipse TE300 microscope, factory set dichroics, and lasers. Fluores-

cence images of cells were recorded under sequential excitation and emission conditions for all probes in a given experiment. All images were processed for background correction, and those of multiple labeled cells for cross-talk correction were processed using Metamorph software (Universal Imaging Corp., West Chester, PA).

**Deletion Analysis of Dynamin**—To generate different domains of dynamin, PCR amplification was performed, and a set of overlapping domains of dynamin was constructed using primer A (5'-CCC GAATT-CATGGGCAACCGCGGC-3'), primer B (5'-GTGGAGGAATTCAAGAACTTCCG-3') primer C (5'-GCAACGAATTCAACAAGAAGAAGACTTC-AGG-3'), primer D (5'-CCGGAATTCGCTCCTTCTGAGGGCTGG-3'), primer E (5'-CTTCTGTCGACTCTGTTGCTCC-3'), primer F (5'-GGTCTCGAGGGCTTTTC-3'), and primer G (5'-GGAATTGACTTGA-CTGCAGG-3') in the indicated combinations: GTPase + middle domain (amino acids 1–505), primers A and E, middle domain (amino acids 313–505), primers B and E; middle domain + PH domain (amino acids 313–636), primers B and F; middle domain + PH domain + GED (amino acids 313–753), primers B and G; PH domain (amino acids 507–636), primers C and F; PH domain + GED (amino acids 507–753), primers C and G; and GED (amino acids 618–753), primers D and G. The PCR products were purified and digested with EcoRI/XhoI or EcoRI/SalI and ligated into compatible ends of the pLexA yeast expression vector.

**NMR Spectroscopy**—For NMR studies, labeled proteins were prepared from *E. coli* BL21 cells harboring the GST-Sumo-1 expression clone grown in M9 minimal medium containing  $^{15}$ NH<sub>4</sub>Cl and  $^{13}$ C-labeled glucose. The culture was induced for protein expression at A<sub>600 nm</sub>  $\sim$  0.6 with 100  $\mu$ M isopropyl- $\beta$ -D-thiogalactopyranoside for 20 h at 28 °C. The harvested culture was lysed in TEND buffer (20 mM Tris (pH 7.4), 5 mM EDTA, 150 mM NaCl, and 1 mM dithiothreitol) containing lysozyme and protease inhibitors. The lysed cells were sonicated and spun at 100,000  $\times$  *g* for 45 min to obtain a clear supernatant. The supernatant was incubated with glutathione-Sepharose beads for 2 h to allow binding of overexpressed recombinant protein. The beads were then washed, and protein was eluted from the column using 20 mM reduced glutathione in TEND buffer (pH 8.0). Protein was dialyzed overnight to remove free glutathione and then subjected to digestion by thrombin to clip off the GST tag. Pure Sumo-1 was obtained by repeatedly passing the digest on the glutathione-Sepharose column.

For NMR experiments, singly labeled ( $^{15}$ N) and doubly labeled ( $^{13}$ C and  $^{15}$ N) Sumo-1 proteins were prepared as described above. The purity and monomeric or oligomeric state of the protein and the homogeneity of the sample were tested by SDS-PAGE analysis and capillary electrophoresis. The proteins were concentrated to  $\sim$ 1 mM and exchanged with TEND buffer (pH 7.4) by ultrafiltration using a 3-kDa cutoff membrane. The final volume of the sample was  $\sim$ 550  $\mu$ l and contained 10% (v/v) D<sub>2</sub>O. Using these proteins, different NMR experiments, *viz.* two-dimensional  $^{15}$ N HSQC and NOESY and three-dimensional HNN and HN(C)N (34, 35), NOESY-HSQC (36), total correlation spectroscopy-HSQC (37), CBCANH (38), CBCANOH (39), and HNC0 (40), were recorded on a Varian 600-MHz NMR spectrometer at 27 °C for resonance assignment and structure determination.

For NMR characterization of the Sumo-GED interaction, 1:1 and 1:2 complexes of Sumo-1 ( $^{15}$ N-labeled) with unlabeled GED were prepared by adding unlabeled GED in small aliquots to a sample of  $\sim$ 1 mM Sumo-1. Two-dimensional HSQC spectra were recorded for both the complexes and were superimposable. This indicated that the interaction was tight on the NMR time scale and stoichiometric; and hence, no further addition of GED was required.

## RESULTS

**Identification of the Members of the Sumoylation Cascade as Interactors of Dynamin**—To identify new interactors of the 100-kDa GTP-binding protein dynamin, a yeast two-hybrid screen was carried out. Since most known interactors of dynamin so far characterized have been identified to interact with the C-terminal PRD of dynamin, we biased our search by using truncated dynamin-1 (lacking the C-terminal PRD) as bait in the screen. A human brain cDNA library was screened using the yeast two-hybrid technique to search for interactors of truncated dynamin (referred to as dynamin $\Delta$ PRD). The screen identified many potential interactors. Two of the clones isolated from the screen encoded full-length Sumo-1, and another two clones represented a fragment of PIAS-1 containing the C-terminal amino acids 396–651. This was significant because

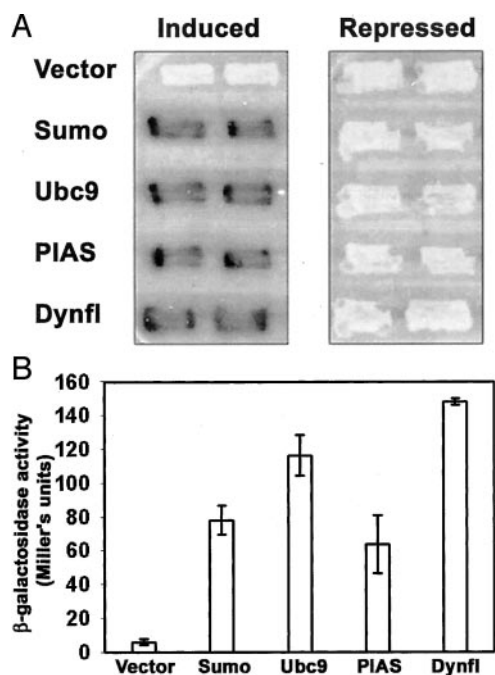


**FIG. 1. Sumoylation machinery proteins interact with dynamin in the yeast two-hybrid system.** *A*, the streaks in duplicate show yeast cells transformed with two-hybrid plasmids grown under induced (*left panel*) and repressed (*right panel*) conditions for reporter gene activation. The streaks represent (from top to bottom) yeast cells cotransformed with pLexA-dynamin $\Delta$ PRD and the pB42AD vector, pB42AD-Sumo-1, pB42AD-Ubc9, pB42AD-PIAS-1(396–651), or pB42AD-dynamin. Dynamin $\Delta$ PRD interacted with Sumo-1, Ubc9, and PIAS-1. The interaction with full-length dynamin (*Dynfl*) was used as a positive control since dynamin is known to oligomerize. *B*, shown is a quantitative representation of the strength of these interactions estimated by liquid culture ONPG assays (see “Experimental Procedures”).

both Sumo (small ubiquitin-related modifier) and PIAS (protein inactivator of undern]activated STAT proteins) are part of the enzymatic cascade constituting sumoylation (24).

The biochemical cascade involving Sumo requires the action of three enzymes referred to as E1, E2, and E3. PIAS-1 has been identified to act as an E3 ligase responsible for the covalent transfer of the 97-amino acid activated Sumo-1 moiety to acceptor lysine residue(s) in target proteins. The E3 ligase is also thought to confer specificity for substrates. We thus decided to focus on these clones and examined the interaction of dynamin with members of the sumoylation cascade more closely. Most interactors of Sumo also show an interaction with Ubc9, the E2 enzyme of the sumoylation cascade. Using the yeast two-hybrid assay, we verified that, in addition to Sumo-1 and PIAS-1, Ubc9 was also an interactor of dynamin $\Delta$ PRD (Fig. 1). As a positive control, we scored the interaction of dynamin $\Delta$ PRD with full-length dynamin.

These interactions were observed by using dynamin fused to the LexA DNA-binding domain vector (pLexA) and members of the sumoylation cascade cloned into the activation domain plasmid (pB42AD). The two plasmids were cotransformed into yeast cells carrying the reporter gene *lacZ*. A positive interaction between two proteins is scored by the activation of the  $\beta$ -galactosidase activity of the *lacZ* reporter gene. As shown in Fig. 1, reporter gene activation was observed in cotransformed yeast cells only under conditions in which expression from the pB42AD plasmid was induced by plating the yeast cells on galactose-containing medium and not when expression from the pB42AD plasmid was repressed by maintaining the yeast cells on glucose-containing medium. As a control, we blunted an EcoRI restriction site in the pLexA-dynamin construct that is located at the extreme 5'-end of the dynamin cDNA, thereby

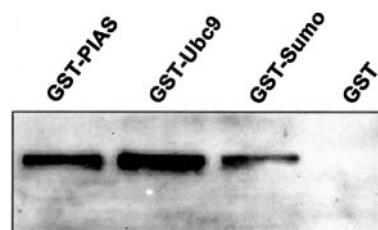


**FIG. 2. Sumoylation machinery proteins pull down dynamin from rat brain lysates.** GST-Sumo-1, GST-Ubc9, GST-PIAS-1(396–651), and GST were immobilized on glutathione-Sepharose beads and incubated with rat brain lysate (50  $\mu$ g of total protein) for 15 min at 4  $^{\circ}$ C to assess their ability to pull down dynamin. Beads thoroughly washed with buffer were boiled in SDS-PAGE sample buffer, and the solubilized proteins were resolved on 11% acrylamide gels. The pulled down dynamin was detected using anti-dynamin-1 primary antibody on Western blots. Dynamin interacted with members of the sumoylation machinery, whereas GST alone did not show any interaction. It was also observed repeatedly that GST-Ubc9 pulled down quantitatively more dynamin compared with the others, which is consistent with the greater strength of the Ubc9-dynamin interaction compared with the Sumo-dynamin and PIAS-dynamin interactions (see Fig. 1*B*). The results shown are representative of at least five such assays.

putting dynamin out of frame with the LexA fusion partner. This abolished the interaction with Sumo-1, Ubc9, and PIAS-1 in the yeast two-hybrid assay (data not shown). This verified that the interaction was indeed dependent on the correct fusion of dynamin-encoding amino acids downstream of the LexA fusion partner.

Since the protein levels induced in yeast cells by the two plasmids are known to be different, we examined the effect of interchanging the vectors on the observed interaction. Sumo-1, Ubc9, and PIAS-1 were ligated into the pLexA vector; dynamin was ligated into the pB42AD vector; and the strength of the interaction was examined using a liquid culture assay for activation of the *lacZ* reporter gene. Although positive interaction could be scored between dynamin and Sumo-1 and between dynamin and Ubc9 using this combination of vectors, the observed strength of interactions was quantitatively weaker than that seen above (data not shown). Also, the pLexA-PIAS-1 construct displayed activation domain-independent reporter gene activation and could thus not be used in these studies. In conclusion, the interactions were more robust and hence more reliably scored when members of the sumoylation cascade were kept in the pB42AD vector. The higher levels of expressed protein from the pB42AD plasmid may account for these differences. All subsequent yeast two-hybrid analyses were thus carried out using Sumo-1, Ubc9, and PIAS-1 in the pB42AD vector with dynamin (or its truncations) ligated into the pLexA plasmid.

*In Vitro Interactions of Dynamin with Sumo-1, Ubc9, and PIAS-1*—To further support the notion that members of the sumoylation cascade interact with dynamin, we examined the ability of purified Sumo-1, Ubc9, and PIAS-1 to interact with dynamin from rat brain lysates using pull-down assays. We expressed Sumo, Ubc9, and the C-terminal part of PIAS-1 comprising amino acids 396–651 in *E. coli* as recombinant proteins containing an N-terminal GST tag. The GST tag allowed these proteins to be immobilized on glutathione-Sepharose beads. Fig. 2 shows that immobilized GST-Sumo-1, GST-Ubc9, and GST-PIAS-1 were able to pull down dynamin from rat brain lysates, whereas immobilized GST alone did not. Upon multiple repetitions of the assay, we observed that Ubc9 was consistently better than Sumo-1 or PIAS-1 in pulling down dynamin. The inclusion of the guanine nucleotide GDP or the non-hydrolyzable analog of GTP did not affect the extent of the pull down (data not shown).

We have thus established the interaction of dynamin with

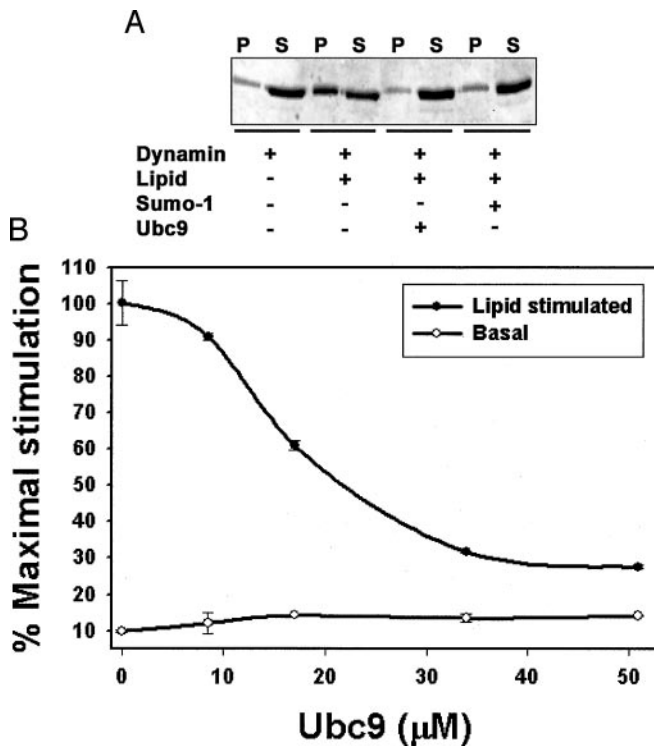


**FIG. 3. Interaction with Sumo-1 and Ubc9 disrupts lipid-mediated oligomerization and GTPase activity of dynamin.** *A*, dynamin was incubated with the indicated components and subjected to ultracentrifugation at  $100,000 \times g$ . Pellet (*P*) and supernatant (*S*) fractions resolved by SDS-PAGE are shown. Oligomerization of dynamin was promoted by the inclusion of lipid ( $50 \mu\text{g/ml}$  phosphatidylserine) as evidenced by more dynamin being present in the *third lane* than in the *first lane*. Further addition of either Sumo-1 or Ubc9 abolished this lipid-mediated oligomerization (*fifth and seventh lanes*). *B*, the effect of Ubc9 addition on basal and lipid-stimulated GTP hydrolysis by dynamin was measured. Inclusion of Ubc9 did not affect basal GTP hydrolysis, but effectively titrated out the lipid-stimulated GTP hydrolysis by dynamin.

Sumo-1, Ubc9, and PIAS-1 using two independent readouts. Additionally, the interaction does not seem to be regulated by the nucleotide (GDP or GTP) bound to dynamin. This is not surprising, as most known interactors of dynamin are insensitive to its nucleotide status.

**Effect of Sumo-1 and Ubc9 on the GTP-hydrolyzing Activity of Dynamin**—To assess the biochemical effect of this interaction on dynamin function, we examined the ability of dynamin to hydrolyze GTP in the presence of Sumo-1 or Ubc9. Dynamin function during endocytosis is critically dependent on the oligomerization of dynamin (8). In contrast with the Ras-like GTPases and the  $\alpha$ -subunits of heterotrimeric GTP-binding proteins, dynamin has a low affinity for GTP and GDP, but a characteristically high rate of GTP hydrolysis (1) that is further stimulated by its lipid-dependent oligomerization (41). Fig. 3*A* (*first through fourth lanes*) shows that inclusion of the lipid phosphatidylserine ( $50 \mu\text{g/ml}$ ) caused oligomerization of dynamin purified from rat brain as judged by the well established ability of oligomerized dynamin to be sedimented at  $100,000 \times g$  (31). In the absence of phosphatidylserine, dynamin was unassembled and thus was present largely in the supernatant (*first and second lanes*), whereas inclusion of  $50 \mu\text{g/ml}$  phosphatidylserine caused oligomerization of dynamin and resulted in its transfer to the pellet fraction after a 15-min spin at  $100,000 \times g$  at  $4^\circ\text{C}$  (*third and fourth lanes*). Inclusion of Sumo-1 or Ubc9 (*fifth through eighth lanes*) interfered with the ability of dynamin to form oligomers in the presence of lipid. Sumo-1 and Ubc9 were recovered in the supernatant

fractions, indicating that they do not bind lipid. Consistent with these observations, Fig. 3*B* shows that whereas basal GTP hydrolysis by dynamin was unaffected by the inclusion of Ubc9 in the assays, lipid-stimulated GTP hydrolysis by dynamin was abolished by titrating in Ubc9 in the reactions. The addition of Sumo-1 instead of Ubc9 had the same effect on GTP hydrolysis (data not shown). Control reactions showed that the inclusion of even 5-fold higher amounts of bovine serum albumin did not perturb the GTP hydrolysis by dynamin. Given the importance of lipid-dependent oligomerization of dynamin for its ability to mediate endocytosis, it was of interest to examine the effect of Sumo-1 and Ubc9 overexpression on cellular endocytosis.

**Overexpression of Sumo-1 in Cells Abrogates Dynamin-dependent Endocytosis**—To test the functional outcome of the sumoylation machinery-dynamin interaction, we overexpressed Sumo-1 and Ubc9 in a mammalian cell line. CHO cells stably expressing the human transferrin receptor are capable of internalizing fluorescently labeled human transferrin. The uptake of transferrin is a dynamin-dependent process, as the expression of dominant-negative dynamin abrogates transferrin uptake in cells (42). We tagged Sumo-1 and Ubc9 with GFP and examined the effect of their overexpression on the uptake of Alexa 568-conjugated human transferrin in these CHO cells. Interestingly, we found that dynamin-mediated uptake of transferrin was abolished in cells overexpressing either GFP-Sumo-1 (Fig. 4*A*) or GFP-Ubc9 (data not shown). In control experiments, we verified that the uptake of labeled transferrin was unaffected in cells expressing GFP alone (data not shown). Fig. 4*A* shows that only the cells expressing GFP-Sumo-1 displayed an inhibition of transferrin uptake, whereas neighboring cells that did not show expression of GFP-Sumo-1 displayed normal transferrin uptake. Thus, consistent with the ability of Sumo and Ubc9 to inhibit the oligomerization of dynamin (seen above), their overexpression in cells serves to down-regulate dynamin-mediated endocytosis most probably by preventing the proper assembly of endogenous dynamin.

It is possible that overexpression of Sumo-1 and Ubc9 in cells might deregulate other cellular processes dependent on sumoylation and that these processes could, in principle, indirectly affect endocytosis. If the observed block in endocytosis is indeed due to interference of overexpressed Sumo-1 (or Ubc9) with the functioning of endogenous dynamin, we reasoned that the block should be relieved by increasing the levels of dynamin in these cells. We thus expressed dynamin-1 in CHO cells. Consistent with other reports (43, 44), overexpression of dynamin did not cause any increased endocytosis of transferrin in CHO cells. We then cotransfected dynamin and GFP-Sumo-1 into CHO cells and examined the uptake of transferrin in doubly transfected cells. As shown in Fig. 4*B*, coexpression of dynamin (*blue*) in cells expressing GFP-Sumo-1 (*green*) resulted in the rescue of transferrin (*red*) uptake. This suggests that the effect of Sumo-1 overexpression on endocytic transferrin uptake is mediated by the action of Sumo-1 on dynamin.

We also examined the effect of Sumo-1 overexpression on an endocytic process not dependent on dynamin. For this purpose, we examined the uptake of RNase A in CHO cells (33). We found that Sumo-1 expression did not interfere with the fluid-phase endocytosis of fluorescently labeled RNase A in these cells (Fig. 4*C*). Cells expressing GFP-Sumo-1 showed amounts of internalized Alexa 555-conjugated RNase A equal to cells not expressing GFP-Sumo-1. These results show that increasing the amount of Sumo-1 in cells serves to specifically down-regulate dynamin-mediated endocytosis with no effect on dynamin-independent fluid-phase endocytosis.

**Dynamin Is Not Sumoylated**—We next asked whether sumoylation of dynamin is responsible for the observed block of

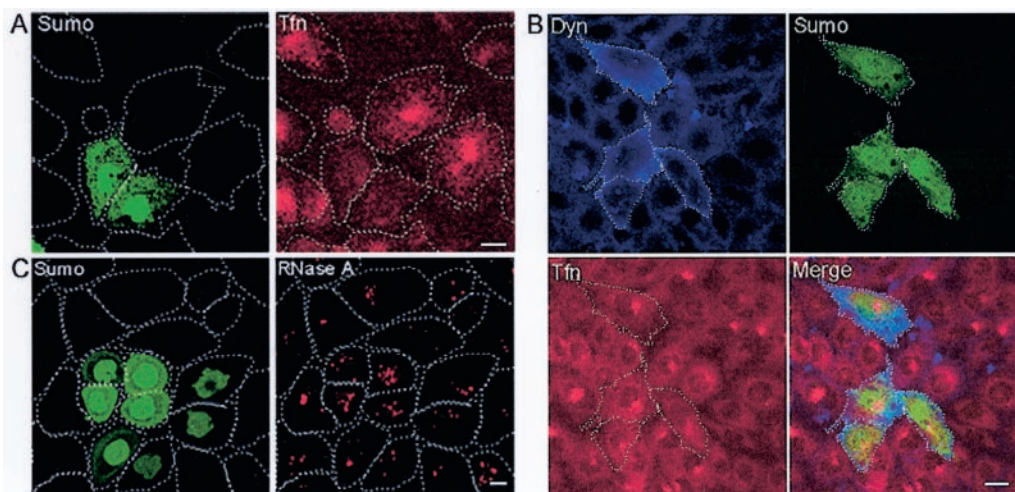


FIG. 4. **Expression of Sumo-1 in CHO cells perturbs dynamin-dependent (but not dynamin-independent) endocytosis.** *A*, cells were transiently transfected with GFP-Sumo-1 (green) and assayed for the dynamin-dependent endocytic uptake of Alexa 568-conjugated transferrin (Tfn; red). Cells expressing GFP-Sumo-1 showed an abrogation of transferrin uptake, whereas neighboring cells not expressing GFP-Sumo-1 showed the characteristic perinuclear distribution of endocytosed transferrin. *B*, the Sumo-1-induced block of endocytosis was rescued by the concurrent expression of dynamin (Dyn). The uptake of transferrin (red) was restored in cells coexpressing Sumo-1 (green) and dynamin (blue). *C*, the dynamin-independent uptake of Alexa 555-conjugated RNase A (red) was unperturbed in cells transiently transfected with GFP-Sumo-1 (green). The uptake of RNase A was the same in all cells. Scale bars = 5  $\mu$ m.

transferrin uptake. Covalent attachment of Sumo to dynamin would result in a modified dynamin species migrating at an apparent molecular mass of  $\sim$ 120 kDa. However, anti-dynamin-1 Western blots of lysates of CHO cells overexpressing either Sumo-1 alone or both Sumo-1 and dynamin-1 showed single bands corresponding to unmodified dynamin-1 and provided no evidence of sumoylated dynamin. Dynamin pulled down from rat brain lysates (or from CHO cells transfected with Sumo and dynamin) using various GST-SH3 domain proteins also did not display any sumoylation.

We have shown that overexpressing the sumoylation machinery in cells results in down-regulation of dynamin-mediated endocytosis. In the normal physiology of the cell, a sharp drop in endocytosis is seen at the time of mitosis (45). To examine whether dynamin sumoylation might underlie this effect, CHO cells were blocked at different stages of the cell cycle. Nocodazole (5  $\mu$ g/ml) was used to arrest cells at the onset of mitosis at the G2/M boundary (46), or alternatively, Taxol (10  $\mu$ g/ml) was used to arrest cells during mitosis (47). Possible dynamin sumoylation was examined by probing cell lysates of these cells with anti-dynamin and anti-Sumo antibodies on Western blots. However, no bands corresponding to the size of sumoylated dynamin were detected.

**The GED of Dynamin Interacts with the Sumoylation Machinery**—To map the interaction site of Sumo-1, Ubc9, and PIAS-1 on dynamin, we constructed a panel of dynamin truncations. Dynamin is a modular protein comprising five domains. Running from the N terminus to the C terminus, these domains are the GTP-binding domain, the middle domain, the PH domain, the GED, and the PRD. We made deletion constructs of dynamin encoding only one or more contiguous domains. These were cloned into the pLexA plasmid, and their interactions with Sumo-1, Ubc9, and PIAS-1 were examined using the yeast two-hybrid assay. The results are summarized in Fig. 5. Only those constructs of dynamin that included the GED showed interaction with members of the sumoylation cascade. The GED alone was also capable of interacting with Sumo-1, Ubc9, and PIAS-1.

We have thus narrowed down the site of interaction of the sumoylation machinery with dynamin to be the GED of dynamin. The GED mediates dynamin oligomerization by GED-GED intermolecular interactions (7). Taken together, our re-

sults suggest that Sumo-1 and Ubc9 interact with the GED, thereby preventing the oligomerization of dynamin. This results in the abrogation of lipid-stimulated GTP hydrolysis by dynamin *in vitro* (Fig. 3) and in the block of dynamin-dependent endocytosis *in vivo* (Fig. 4).

We then wondered whether expression of the dynamin GED alone in cells could rescue the block of dynamin-dependent endocytosis induced by the overexpression of GFP-Sumo-1. We constructed Myc-tagged dynamin GED and overexpressed it in CHO cells. Control experiments established that expression of Myc-GED did not perturb the uptake of Alexa 568-conjugated transferrin in these cells. We next co-transfected plasmids expressing GFP-Sumo-1 and Myc-GED into CHO cells. Whereas GFP-Sumo-1-expressing cells were impaired in transferrin uptake, cells coexpressing GFP-Sumo-1 and Myc-GED exhibited normal endocytic uptake of transferrin (data not shown). These results support the observation that the GED of dynamin is the site of noncovalent interaction with the sumoylation machinery.

**Identification of the Surface on Sumo-1 That Interacts with the GED of Dynamin**—Further characterization of the interaction of the dynamin GED with Sumo-1 was obtained by high resolution NMR experiments. The two-dimensional HSQC spectrum of a protein represents its “fingerprint” in the sense that every amino acid residue produces one backbone amide proton and  $^{15}$ N correlation peak in the spectrum. The position of every peak is very sensitive to its local environment and hence is a convenient monitor for residue-specific changes due to complex formation with ligands or other proteins (48).

Fig. 6A shows the two-dimensional HSQC spectrum (black) of free  $^{15}$ N-labeled Sumo-1. Sequence-specific assignment of the individual peaks was obtained by procedures based on triple resonance three-dimensional HNN and HN(C)N experiments. Fig. 6B shows an illustrative sequential walk for the stretch Gly<sup>19</sup>–Lys<sup>25</sup> through the HNN spectrum, which allows assignment of amide proton and  $^{15}$ N chemical shifts of specific residues. All the peaks in Fig. 6A were thus assigned.

The addition of unlabeled GED to the Sumo-1 sample caused small but reproducible shifts in the positions of the peaks. The spectrum of the 1:1 complex of Sumo and GED is shown in red (Fig. 6A) superposed on the spectrum of Sumo alone (black) to display residue-specific changes in the peak positions. Clearly,

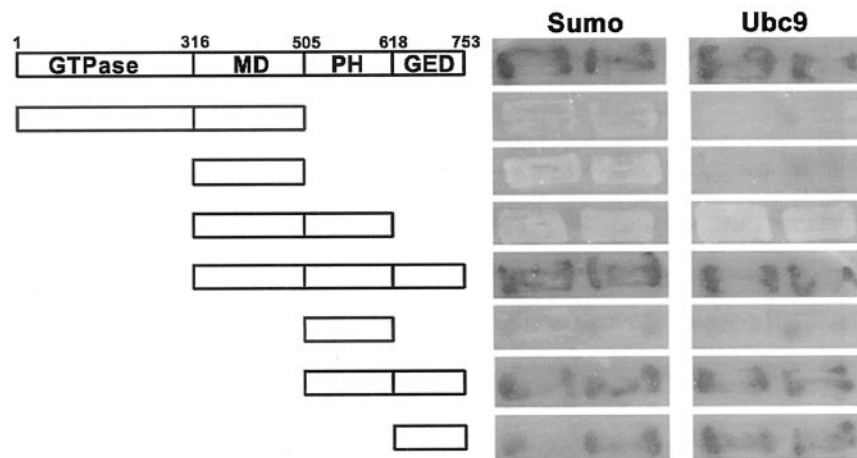


**FIG. 5. Deletion analysis of dynamin identified the GED as the site of interaction with Sumo-1 and Ubc9.** Dynamin $\Delta$ PRD was identified as interacting with the sumoylation machinery. The site of interaction on dynamin was further narrowed down by cloning the various domains of dynamin either singly or in combination into the pLexA plasmid and testing their interaction with Sumo-1 and Ubc9 cloned into pB42AD. The domains of dynamin are as follows: GTPase domain (amino acids 1–316), middle domain (MD; amino acids 313–505), PH domain (amino acids 505–636), and GED (amino acids 618–753). The proline/arginine-rich domain (amino acids 750–864) was not considered here because the interaction was uncovered using dynamin $\Delta$ PRD as bait. It is readily seen that only constructs containing the GED were able to interact with Sumo-1 and Ubc9. In fact, the GED alone was able to recapitulate the interaction with the sumoylation machinery.

different residues show shifts to varying degrees, which is an indication of the specificity of the interaction; the amino acid residues corresponding to those peaks that show large changes have been labeled. The peak shifts for all the residues have been quantified and are shown in Fig. 6C. The residues that show significant shifts (larger than  $\sim 0.1$  ppm) were clearly strongly influenced by GED binding and hence identify the binding surface of the protein (49). Thus, we conclude that Ile<sup>22</sup>, Lys<sup>23</sup>, Leu<sup>65</sup>, Phe<sup>66</sup>, Glu<sup>67</sup>, Gly<sup>68</sup>, Arg<sup>70</sup>, Ala<sup>72</sup>, Leu<sup>80</sup>, Gly<sup>81</sup>, Met<sup>82</sup>, Glu<sup>83</sup>, Val<sup>87</sup>, Ile<sup>88</sup>, and Glu<sup>89</sup> of Sumo-1 are responsible for its interaction with the GED of dynamin.

Next, to determine the topology of the binding surface of Sumo-1, we determined the three-dimensional structure of the protein under the same pH and temperature experimental conditions (pH 7.4 and 27 °C) as used for the interaction studies; previous studies have investigated the structure and dynamics of Sumo-1 under somewhat different experimental conditions (50, 51). For this, we first obtained the assignments of H $\alpha$ , C $\alpha$ , C $\beta$ , and CO from a combination of total correlation spectroscopy-HSQC, CBCANH, CBCACONH, and HNCOC experiments. The structure of the molecule was then determined by DYANA calculations (52) using 585 distance constraints derived from two-dimensional NOESY and three-dimensional NOESY-HSQC spectra; 126 dihedral ( $\phi$ ,  $\psi$ ) constraints derived from the TALOS algorithm (53) using <sup>15</sup>N, H $\alpha$ , C $\alpha$ , C $\beta$ , and CO chemical shifts; and 48 H-bond distance constraints derived from deuterium exchange measurements. Fig. 6D shows the structure of the molecule thus derived as a ribbon diagram. Sumo-1 consists of five  $\beta$ -sheets ( $\beta$ 1– $\beta$ 5) and two  $\alpha$ -helices ( $\alpha$ 1 and  $\alpha$ 2), with helix  $\alpha$ 2 being relatively disordered. This structure is essentially similar to that reported by Bayer *et al.* (54) with regard to secondary structure elements, but has differences in the overall organization of these elements. It appears that the structure and dynamics of Sumo-1 are quite sensitive to experimental conditions, and the details of such structural and dynamic characterizations will be reported separately.

Residues on Sumo-1 forming the binding surface between Sumo-1 and GED have been highlighted in Fig. 6D. Ile<sup>22</sup> and Lys<sup>23</sup> lie at the beginning of the first  $\beta$ -sheet, and Leu<sup>65</sup>–Gly<sup>68</sup>, Arg<sup>70</sup>, and Ala<sup>72</sup> lie in the loop between  $\beta$ 3 and  $\beta$ 4. Leu<sup>80</sup>–Glu<sup>83</sup> lie in the loop following the mobile helix  $\alpha$ 2, and Val<sup>87</sup>–Glu<sup>89</sup> lie at the beginning of  $\beta$ 5. Overall, these residues constitute a relatively flexible pocket, suggesting that small conformational

perturbations within Sumo-1 could easily regulate the interaction between Sumo-1 and the GED of dynamin.

#### DISCUSSION

In this study, we have identified the 100-kDa endocytic GTP-binding protein dynamin as an interactor of the sumoylation machinery. The GED has been identified as the site on dynamin that engages the sumoylation machinery. Although we have no evidence for the covalent attachment of Sumo-1 to dynamin, we have shown that overexpressing Sumo-1 and Ubc9 in mammalian cells results in down-regulation of dynamin-dependent endocytosis of transferrin. This effect is consistent with our observation that Sumo-1 and Ubc9 abolish the oligomerization of dynamin possibly by sequestering unassembled dynamin.

It is interesting that the structurally analogous GTP-binding Mx proteins have also been shown to interact with Sumo-1 (55). However, covalent attachment of Sumo to the Mx proteins has not been demonstrated. The septins Cdc3, Cdc11, and Shs1 have also been shown to be sumoylated in a cell cycle-dependent manner (46). Septins are GTP-binding coiled-coil proteins that are involved in cytokinesis in the budding yeast *Saccharomyces cerevisiae* and, like dynamin, are known to mediate scission events by forming spiral structures (56) around the yeast bud necks. Sumoylation of the septins occurs shortly before the onset of anaphase, and desumoylation occurs abruptly at cytokinesis (46). We searched for an analogous stage in the cell cycle for the possible sumoylation of dynamin in mammalian cells grown in culture. However, no evidence of the covalent attachment of Sumo-1 to dynamin was seen in CHO cells that were arrested either before the onset of mitosis (by nocodazole) or in late mitosis (blocked in cytokinesis by Taxol).

Sumoylation has been shown to occur on many (although not all) substrates at lysine residues that lie within a consensus  $\psi$ KXE motif (where  $\psi$  is a hydrophobic amino acid, X is any amino acid, and E is an acidic amino acid) (57). The amino acid sequence of dynamin has the stretch VK<sup>376</sup>ME in the middle domain corresponding to this consensus motif. We found that peptides containing this sequence (PFELVKMEFDE) do get sumoylated *in vitro* (data not shown). However, we have not been able to observe the sumoylation of the isolated middle domain of dynamin when expressed as a recombinant protein

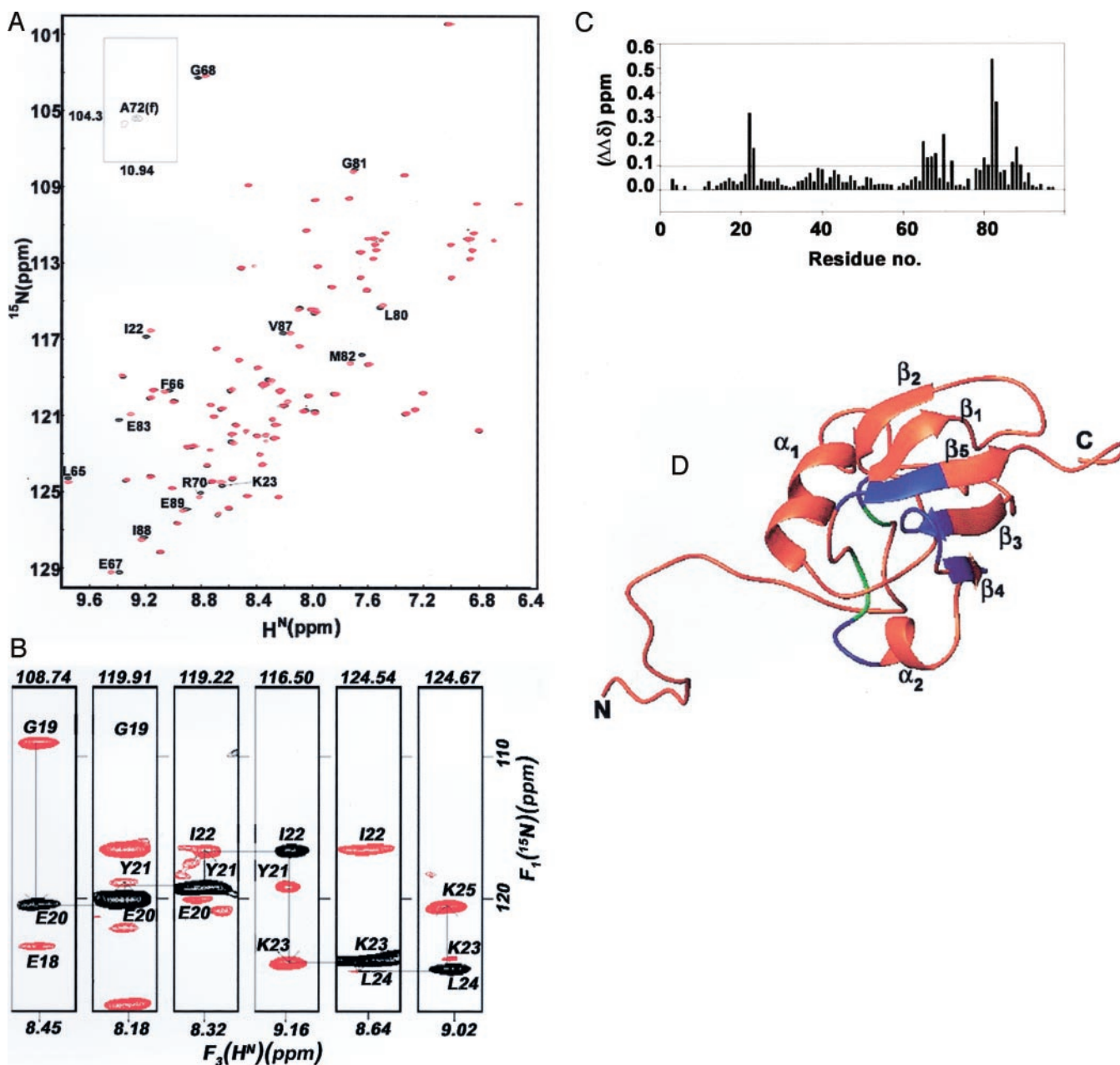


**FIG. 6. Analysis of the Sumo-GED interaction using NMR.** *A*, superposition of the  $^1\text{H}$ - $^{15}\text{N}$  HSQC spectra of  $^{15}\text{N}$ -labeled Sumo-1 free (*black*) and in complex with unlabeled GED (*red*). The Sumo-1/GED ratio in the complex was  $\sim 1:1$ . Peaks showing considerable shifts upon complex formation have been labeled. The folded peak of Ala<sup>72</sup>, which occurs at a distinctly different region of the spectrum, is shown in the *inset*. *B*, illustrative sequential walk through the  $F_1$ - $F_3$  planes in the HN spectrum of Sumo-1 at pH 7.4 and 300 K. Sequential connectivities are indicated for the stretch Gly<sup>19</sup>-Lys<sup>25</sup> along the protein primary sequence. Strips from the relevant planes at appropriate  $H^N$  chemical shifts are shown. *C*, average chemical shift change ( $\Delta\Delta\delta$ ) versus residue number of  $^{15}\text{N}$ -labeled Sumo-1 upon complex formation with unlabeled GED. The average chemical shift changes for the individual residues were calculated as  $(5\Delta\delta_{\text{HN}})^2 + (\Delta\delta_{\text{N}})^2)^{1/2}$ , where  $\Delta\delta_{\text{HN}}$  and  $\Delta\delta_{\text{N}}$  are the perturbations in amide proton and  $^{15}\text{N}$  chemical shifts for each residue, respectively. A *horizontal line* has been drawn at a threshold of 0.1 ppm to highlight those residues that were most affected upon complex formation. *D*, ribbon diagram of the NMR-derived Sumo-1 structure.  $\beta_1$ - $\beta_5$  are the  $\beta$ -sheets, and  $\alpha_1$  and  $\alpha_2$  are the helices in the structure. The residues that showed significant chemical shift perturbations upon binding with GED have been color-coded. Those that showed chemical shift changes  $>0.2$  ppm are in *green*, and others are in *blue*. Together, these identify the binding surface for GED on Sumo-1.

in bacteria or the *in vitro* sumoylation of full-length dynamin purified from rat brain. We are currently mutating Lys<sup>376</sup> in dynamin and will express the mutant protein in mammalian cells to test the importance of this site.

It is possible that we have not found the correct conditions under which dynamin may be sumoylated. The functions of dynamin are regulated by various phosphorylation events, and it may be that dynamin is sumoylated only under a specific set of circumstances. On the other hand, it is conceivable that dynamin does not act as a covalent acceptor of Sumo-1, but that

it serves to concentrate the sumoylation machinery at its GED, thereby facilitating the sumoylation of some other substrate(s). These substrates might be interactors of dynamin. It is of interest to note in this regard that a recent report has provided evidence for the nucleocytoplasmic shuttling of some endocytic proteins (58). Eps15, epsin, clathrin assembly lymphoid myeloid leukemia protein, and  $\alpha$ -adaptin, all of which are significantly larger in size than proteins that freely diffuse through nuclear pores, were seen to be sequestered in the nuclei of cells blocked in nuclear export. However, no mechanism for the

nuclear translocation of these normally cytoplasmic proteins has been identified. Our results raise the intriguing possibility that sumoylation could mediate the nuclear transport of these endocytic proteins. These proteins are all known to interact with dynamin, and their sumoylation could conceivably be facilitated by concentrating the sumoylation machinery on dynamin. Efforts are currently underway in our laboratory to test this hypothesis.

Many proteins involved in endocytosis (some of which are interactors of dynamin) are known to be ubiquitinated or to possess ubiquitin-interacting motifs (59, 60). The ubiquitination of some of these proteins may be regulated by competing dynamin-facilitated sumoylation. An example of such competition between Sumo and ubiquitin has been reported, where the sumoylation of the transcriptional regulator I $\kappa$ B $\alpha$  prevented its ubiquitination and subsequent proteasomal degradation (61).

The best characterized function of ubiquitination is to target ubiquitinated proteins for proteasomal degradation, although proteasome-independent events such as changes in protein localization and activity are also being uncovered (62). Monoubiquitination is being appreciated as an important regulator of endocytosis (63). Sumoylation may play a part in endocytosis by acting as an antagonist of some of these monoubiquitination events. Sumoylation is known to enhance the stability of its target proteins or to modulate their subcellular localization (25). Even more striking are the growing number of reports suggesting that noncovalent interactions of Sumo with a number of molecules may also be of biological significance (27, 28, 29).

Dynamin has also gained recognition as a molecule whose activity is required for the activation of the MAPK cascade subsequent to the engagement of cell-surface G-protein-coupled receptors (64, 65). The exact role of dynamin in this pathway is still open to debate. It is clear, however, that dynamin function is not required at the level of G-protein-coupled receptor internalization (66). It is currently postulated that dynamin function is required for the correct translocation of activated MEK in cells. Significantly, it has been shown in *Dictyostelium* cells that MEK localization is controlled by a tightly regulated cycle of sumoylation-desumoylation (67). It is conceivable that MEK sumoylation could be facilitated by dynamin acting as a scaffold for the sumoylation machinery. However, it remains to be established whether the sumoylation of MEK is a general phenomenon occurring in mammalian cells and, if so, whether dynamin is involved in this process. The involvement of dynamin in the activation of the MAPK cascade could thus require a non-endocytic role for dynamin. This possibility is also being currently investigated in our laboratory.

This study is an initial characterization of the interaction of dynamin with the sumoylation machinery. Using various independent readouts, we have established the GED of dynamin as being an interacting site for Sumo-1, Ubc9, and PIAS-1. Furthermore, using high resolution NMR, we have identified the residues on Sumo-1 that interact with the GED of dynamin. Interestingly, the residues on Sumo-1 that participate in its interaction with the GED are partially the same as those that interact with Ubc9 (49).<sup>2</sup> This suggests that the interaction of Sumo-1 with Ubc9 and GED might occur sequentially rather than simultaneously. We speculate that dynamin could conceivably then act as an adapter E3 molecule for the transfer of Sumo to an acceptor lysine residue. Such a role has been postulated for the polycomb Pc2 protein (26). Ongoing studies are examining the effects of mutation of these residues on

Sumo-dynamin interactions. The physiological relevance of the Sumo-dynamin interaction has yet to be understood fully, and efforts are currently underway to examine signaling events downstream of G-protein-coupled receptor activation in Sumo-1-overexpressing cells.

**Acknowledgments**—We gratefully acknowledge Prof. Ronald T. Hay for the generous gift of plasmids encoding GST-SAE1/2 (used in *in vitro* sumoylation assays) and GST-Ubc9; Prof. Kay Shuai (UCLA) for a plasmid encoding GST-mouse PIAS; Prof. Frauke Melchior (Max-Planck-Institut, Martinsried, Germany) for a plasmid for RanGAP (used as a positive control in *in vitro* sumoylation assays); Dr. Vidita Vaidya (Tata Institute of Fundamental Research) for rat brains; and Prof. Alfred Wittinghofer (Max-Planck-Institut, Dortmund, Germany) for numerous reagents and encouragement.

## REFERENCES

1. Praefcke, G. J. K., and McMahon, H. T. (2004) *Nat. Rev. Mol. Cell. Biol.* **5**, 133–147. G. J. K.
2. Conner, S. D., and Schmid, S. L. (2003) *Nature* **422**, 37–44
3. McNiven, M. A., Cao, H., Pitts, K. R., and Yoon, Y. (2000) *Trends Biochem. Sci.* **25**, 115–120
4. Henley, J. R., Krueger, E. W., Oswald, B. J., and McNiven, M. A. (1998) *J. Cell Biol.* **141**, 85–99
5. Haller, O., and Kochs, G. (2002) *Traffic* **3**, 710–717
6. van der Blik, A. M. (1999) *Trends Cell Biol.* **9**, 96–102
7. Okamoto, P. M., Triplet, B., Litowski, J., Hodges, R. S., and Vallee, R. B. (1999) *J. Biol. Chem.* **274**, 10277–10286
8. Sever, S., Muhlberg, A. B., and Schmid, S. L. (1999) *Nature* **398**, 481–486
9. Schmidt, A., Wolde, M., Thiele, C., Fest, W., Kratzin, H., Podtelebnikov, A. V., Witke, W., Huttner, W. B., and Soling, H. D. (1999) *Nature* **401**, 133–141
10. Song, B. D., and Schmid, S. L. (2003) *Biochemistry* **42**, 1369–1376
11. Stowell, M. H., Marks, B., Wigge, P., and McMahon, H. T. (1999) *Nat. Cell Biol.* **1**, 27–32
12. Smirnova, E., Shurland, D. L., Newman-Smith, E. D., Pishvae, B., and van der Blik, A. M. (1999) *J. Biol. Chem.* **274**, 14942–14947
13. Muhlberg, A. B., Warnock, D. E., and Schmid, S. L. (1997) *EMBO J.* **16**, 6676–6683
14. Vallis, Y., Wigge P., Marks, B., Evans, P. R., and McMahon, H. T. (1999) *Curr. Biol.* **9**, 257–260
15. Lin, H. C., and Gilman, A. G. (1996) *J. Biol. Chem.* **271**, 27979–27982
16. Tan, T. C., Valova, V. A., Malladi, C. S., Graham, M. E., Berven, L. A., Jupp, O. J., Hansra, G., McClure, S. J., Sarcovic, B., Boadle, R. A., Larsen, M. R., Cousin, M. A., and Robinson, P. J. (2003) *Nat. Cell Biol.* **5**, 701–710
17. Hinshaw, J. E. (2000) *Annu. Rev. Cell Dev. Biol.* **16**, 483–519
18. Wang, L. H., Sudhof, T. C., and Anderson, R. G. (1995) *J. Biol. Chem.* **270**, 10079–10083
19. Baillat, G., Gaillard, S., Castets, F., and Monneron, A. (2002) *J. Biol. Chem.* **277**, 18961–18966
20. Newmyer, S. L., Christensen, A., and Sever, S. (2003) *Dev. Cell* **4**, 929–940
21. Fields, S., and Song, O. (1989) *Nature* **340**, 245–246
22. Schwartz, D. C., and Hochstrasser, M. (2003) *Trends Biochem. Sci.* **28**, 321–328
23. Seeler, J. S., and Dejean, A. (2003) *Nat. Rev. Mol. Cell. Biol.* **4**, 690–699
24. Melchior, F., Schergaut, M., and Pichler, A. (2003) *Trends Biochem. Sci.* **28**, 612–618
25. Mueller, S., Hoege, C., Pyrowolakis, G., and Jentsch, S. (2001) *Nat. Rev. Mol. Cell. Biol.* **2**, 202–210
26. Kagey, M. H., Melhuish, T. A., and Wotton, D. (2003) *Cell* **113**, 127–137
27. Kaukinen, P., Vaheri, A., and Plyusnin, A. (2003) *Virus Res.* **92**, 37–45
28. Maeda, A., Lee, B. H., Yoshimatsu, K., Saijo, M., Kurane, I., Arikawa, J., and Morikawa, S. (2003) *Virology* **305**, 288–297
29. Li, W., Hesabi, B., Babbo, A., Pacione, C., Liu, J., Chen, D. J., Nickloff, J. A., and Shen, Z. (2000) *Nucleic Acids Res.* **28**, 1145–1153
30. Gyuris, J., Golemis, E., Chertkov, H., and Brent, R. (1993) *Cell* **75**, 791–803
31. Hinshaw, J. E., and Schmid, S. L. (1995) *Nature* **374**, 190–192
32. Mayor, S., Presley, J. F., and Maxfield, F. R. (1993) *J. Cell Biol.* **121**, 1257–1269
33. Haigis, M. C., and Raines, R. T. (2003) *J. Cell Sci.* **116**, 313–324
34. Panchal, S. C., Bhavesh, N. S., and Hosur, R. V. (2001) *J. Biomol. NMR* **20**, 135–147
35. Bhavesh, N. S., Panchal, S. C., and Hosur, R. V. (2001) *Biochemistry* **40**, 14727–14735
36. Marion, D., Driscoll, P. C., Kay, L. E., Wingfield, P. T., Bax, A., Gorenborn, A. M., and Clore, G. M. (1989) *Biochemistry* **28**, 6150–6156
37. Grzesick, S., and Bax, A. (1993) *Acc. Chem. Res.* **26**, 131–138
38. Grzesick, S., and Bax, A. (1992) *J. Magn. Reson.* **99**, 201–207
39. Grzesick, S., and Bax, A. (1992) *J. Am. Chem. Soc.* **114**, 6291–6293
40. Kay, L. E., Ikura, M., Tscudin, R., and Bax, A. (1990) *J. Magn. Reson.* **89**, 496–514
41. Tuma, P. L., Stachniak, M. C., and Collins, C. A. (1993) *J. Biol. Chem.* **268**, 17240–17246
42. van der Blik, A. M., Redelmeier, T. E., Damk, H., Tisdale, E. J., Meyerowitz, E. M., and Schmid, S. L. (1993) *J. Cell Biol.* **122**, 553–563
43. Damke, H., Baba, T., Warnock, D. E., and Schmid, S. L. (1994) *J. Cell Biol.* **127**, 915–934
44. Achiriloaie, M., Barylko, B., and Albanesi, J. P. (1999) *Mol. Cell. Biol.* **19**, 1410–1415
45. Pypaert, M., Mundy, D., Souter, E., Labbe, J. C., and Warren, G. (1991) *J. Cell Biol.* **114**, 1159–1166

<sup>2</sup> R. K. Mishra, S. S. Jatiani, A. Kumar, V. R. Simhadri, R. V. Hosur, and R. Mittal, unpublished data.

46. Johnson, E. S., and Blobel, G. (1999) *J. Cell Biol.* **147**, 981–993
47. Vorobjev, I. A., Uzbekov, R. E., Komarova, Y. A., and Alieva, I. B. (2000) *Membr. Cell Biol.* **14**, 219–235
48. Shuker, S. B., Hajduk, P. J., Meadows, R. P., and Fesik, S. W. (1996) *Science* **274**, 1531–1534
49. Lin, D., Tatham, M. H., Yu, B., Kim, S., Hay, R. T., and Chen, Y. (2002) *J. Biol. Chem.* **277**, 21740–21748
50. Liu, Q., Jin, C., Liao, X., Shen, Z., Chen, D. J., and Chen, Y. (1999) *J. Biol. Chem.* **274**, 16979–16987
51. Jin, C., Shiyanova, T., Shen, Z., and Liao, X. (2001) *Int. J. Biol. Macromol.* **28**, 227–234
52. Guntert, P., Mumenthaler, C., and Wuthrich, K. (1997) *J. Mol. Biol.* **273**, 283–298
53. Cornilescu, G., Delaglio, F., and Bax, A. (1999) *J. Biomol. NMR* **13**, 289–302
54. Bayer, P., Arndt, A., Metzger, S., Mahajan, R., Melchior, F., Jaenicke, R., and Becker, J. (1998) *J. Mol. Biol.* **280**, 275–286
55. Engelhardt, O. G., Ullrich, E., Kochs, G., and Haller, O. (2001) *Exp. Cell Res.* **271**, 286–295
56. Longtine, M. S., and Bi, E. (2003) *Trends Cell Biol.* **13**, 403–409
57. Sampson, D. A., Wang, M., and Matunis, M. J. (2001) *J. Biol. Chem.* **276**, 21664–21669
58. Vecchi, M., Polo, S., Poupon, V., van de Loo, J. W., Benmerah, A., and Di Fiore, P. P. (2001) *J. Cell Biol.* **153**, 1511–1517
59. Haglund, K., Di Fiore, P. P., and Dikic, I. (2003) *Trends Biochem. Sci.* **28**, 598–603
60. Wojcikiewicz, R. J. (2004) *Trends Pharmacol. Sci.* **25**, 35–41
61. Desterro, J. M., Rodriguez, M. S., and Hay, R. T. (1998) *Mol. Cell* **2**, 233–239
62. Pickart, C. M. (2001) *Annu. Rev. Biochem.* **70**, 503–533
63. Li, M., Brooks, C. L., Wu-Baer, F., Chen, D., Baer, R., and Gu, W. (2003) *Science* **302**, 1972–1975
64. Ahn, S., Maudsley, S., Luttrell, L. M., Lefkowitz, R. J., and Daaka, Y. (1999) *J. Biol. Chem.* **274**, 1185–1188
65. Kranenburg, O., Verlaan, I., and Moolenaar, W. H. (1999) *J. Biol. Chem.* **274**, 35301–35304
66. Whistler, J. L., and von Zastrow, M. (1999) *J. Biol. Chem.* **274**, 24575–24578
67. Sobko, A., Ma, H., and Firtel, R. A. (2002) *Dev. Cell* **2**, 745–756